JOURNAL OF NEUROTRAUMA 36:61–73 (January 1, 2019)

DOI: 10.1089/neu.2017.5551

Controlled Cortical Impact Severity Results in Graded Cellular, Tissue, and Functional Responses in a Piglet Traumatic Brain Injury Model

Emily W. Baker,[1,2,*] Holly A. Kinder,[1,2,*] Jessica M. Hutcheson,[1,2] Kylee Jo J. Duberstein,[1,2] Simon R. Platt,[1,3] Elizabeth W. Howerth,[1,4] and Franklin D. West[1,2]

Abstract

A number of pre-clinical rodent models have been developed in an effort to recapitulate injury mechanisms and identify potential therapeutics for traumatic brain injury (TBI), which is a major cause of death and long-term disability in the United States. The lack of restorative treatments for TBI, however, has led to considerable criticism of current pre-clinical therapeutic development strategies—namely, the translatability of widely used rodent models to human patients. The use of large animal models, such as the pig, with more brain anatomy and physiology comparable to humans may enhance the translational capacity of current pre-clinical animal models. The objective of this study was to develop and characterize a graded piglet TBI model with quantitative pathological features at the cellular, tissue, and functional level that become more prominent with increasing TBI severity. A graded TBI was produced by controlled cortical impact (CCI) in ''toddler-aged'' Landrace piglets by increasing impact velocity and/or depth of depression to 2 m/sec; 6 mm; 4 m/sec; 6 mm; 4 m/sec; 12 mm; or 4 m/sec; 15 mm, producing a range of neural injury responses that corresponded to injury severity. Quantitative gait analysis was performed pre-TBI and one, three, and seven days post-TBI, and piglets were sacrificed seven days post-TBI. Increasing impact parameters correlated to increases in lesion size with piglets that sustained a 6 mm depth of depression exhibiting significantly smaller lesions than piglets that sustained a depth of depression of 12 mm or 15 mm. Similarly, the extent of neuronal loss, astrogliosis/astrocytosis, and white matter damage became more prominent as CCI parameters were increased. These cellular and tissue-level changes correlated with motor function deficits including swing/stance time, stride velocity, and two- versus three-limb support. The piglet TBI model described here could serve as a translational platform for studying TBI sequelae across injury severities and identifying novel therapeutics.

Keywords: controlled cortical impact; functional impairment; pig models; traumatic brain injury

Introduction

In the United States, traumatic brain injury (TBI) results in an estimated 2174 deaths and 473,947 emergency department visits among children aged 0–14 years annually.[1] Falls account for approximately 50.2% of all sustained TBIs for children, and the rate of fall-related TBIs is highest among children aged 0–4 years (839 per 100,000).[1] Further, pediatric TBI accounts for more than $1 billion in total hospital charges annually.[2] Although adolescent brains are believed to be more ''plastic'' and thus more adept to recover and restore function after injury, recent evidence has shown that children who sustain a TBI at a younger age may have long-term neurological consequences such as impairments in cognition, behavior, and motor function.[3–7]

At present, a number of management strategies are utilized to monitor and alter critical aspects affecting TBI outcomes including intracranial pressure, cerebral oxygenation, cerebral edema, and cerebrovascular injury after pediatric TBI, which may substantially decrease hospital stays and mortality rates.[8] Treatment options are restricted to techniques such as hyperosmolar therapy, temperature control, cerebrospinal fluid drainage, barbiturate therapy, and decompressive craniectomy that aim to reduce secondary brain insults.[9] Despite these treatments, many patients still experience significant long-term functional deficits leading to a major need for better therapies.[10–12]

Numerous experimental rodent models have been developed in an effort to recapitulate the primary and secondary injury aspects of a human TBI and, in turn, have helped delineate many of the

[1]Regenerative Bioscience Center, [2]Department of Animal and Dairy Science, [3]Department of Small Animal Medicine and Surgery, [4]Department of Pathology, College of Veterinary Medicine, University of Georgia, Athens, Georgia.
*E.W.B. and H.A.K. contributed equally to this work.

biomechanical, cellular, molecular, and functional responses of TBI that cannot be studied in a clinical setting.[13] In rodents, one of the most widely used and studied TBI models is the controlled cortical impact (CCI) model. CCI allows for precise, quantitative control over parameters that affect injury severity such as velocity, depth of depression, and tip diameter.[14] CCI can be manipulated to produce injuries ranging from mild to severe and is highly reproducible.[15] The ability to control injury severity allows researchers to produce gradable tissue damage, functional impairments, provide a means to better account for the variation in pathologies observed in TBI patients, and most importantly, develop appropriate treatment strategies.[14]

Magnetic resonance imaging (MRI) studies in pediatric patients with TBI have revealed that lesion size, gray and white matter disruption, and brain atrophy can be influenced by injury severity.[16] Functional deficits, such as cognition and motor function, have been documented to vary according to injury severity in children after TBI.[17,18] To address this, graded CCI rodent models have been used to characterize the effects of injury severity on histopathological changes and behavioral and motor responses after injury and, consequently, to identify potential therapeutic targets.[19–23]

Despite promising pre-clinical results in rodent studies utilizing a wide range of therapeutics, there is no Food and Drug Administration approved treatment that promotes functional recovery in humans.[24–26] Given the significant impact of TBI, particularly in children who are at a critical period of brain development, the lack of effective treatments has led to considerable criticism of the use of rodents as a translational model.[27,28]

The pig, having similarities in brain anatomy and physiology to humans, may provide a significant advantage in modeling TBI and testing the safety and efficacy of novel therapeutics. The human brain is gyrencephalic and comprises >60% white matter.[29,30] The gyrencephalic piglet brain has been found to mirror the pediatric brain in terms of size, development, and neuroinflammatory response, and also comprises >60% white matter.[31–34] The lissencephalic rodent brain, however, is 650 times smaller than the human brain and is composed of only 14% of the relative white matter volume of humans.[30,35–37] Given the propensity for TBI to contribute to widespread white matter damage in human patients, the use of a large animal model with comparable white matter composition and a gyrencephalic brain is critical to more closely recapitulate the human pathology.[38]

To date, a number of large animal CCI models have been developed in ferrets,[39–41] monkeys,[42] and swine.[43–45] Despite increasing interest in studying focal brain trauma in more large animal models of TBI, a limited number of groups have pursued CCI piglet models.[43,46] Further, studies that directly examine the effects of injury severity on cellular and tissue dynamics and corresponding motor function responses in a piglet CCI model are lacking.[43,45]

The purpose of this study was to develop and characterize a piglet TBI model with graded severity by manipulating CCI velocity, depth of depression, or both and measuring corresponding changes at the cellular, tissue, and functional levels. Lesion size and histological analysis were assessed to measure changes at the tissue and cellular level and were found to correlate with injury severity. In addition, spatial-temporal gait analysis was performed to assess changes in motor function and was found to respond as a function of increasing injury severity. The development of a piglet TBI model with pathological and functional changes that mirror human patients with TBI can be used in future studies to serve as a platform for the testing of novel therapeutics.

Methods

All work performed in this study was done in accordance with the University of Georgia Institutional Animal Care and Use Committee guidelines.

Animals

Sixteen commercially bred Landrace-cross piglets of mixed sex and three weeks of age were obtained from the University of Georgia Swine Unit one week before the surgical procedure. Piglets were group housed and fed a nutritionally complete starter diet *ad libitum.* Room temperature was maintained at 26°C with a 12 h light/dark cycle, and an overhead heat lamp provided supplemental heat. All animals were feed restricted overnight before operation but had free access to water.

Surgical preparation

Piglets underwent the surgical procedure at four weeks of age. Anesthesia was induced using 5% vaporized isoflurane in oxygen utilizing a surgical mask. After induction, anesthesia was maintained at 2–3% vaporized isoflurane in oxygen via nose cone. Continuous physiological monitoring of heart rate, respiration rate, and rectal temperature was performed every 5 min after induction of anesthesia. A target temperature range of 99–102°F was maintained using blankets and a heating pad. The skin was prepared in a routine manner for sterile surgery using Betadine and 70% alcohol. The surgical site was draped in a standard fashion. A left-sided skin incision approximately 4 cm in length was made over the top of the cranium, and soft tissues were dissected away to expose the skull. An air drill (Brasseler) was used to produce a circular craniectomy approximately 20 mm in diameter at the left posterior junction of the coronal and sagittal sutures (Supplementary Fig. 1; see online supplementary material at ftp.liebertpub.com). Care was taken to avoid disruption of the dura mater and underlying cortical surface.

CCI

Concussive TBI was generated through the use of a specialized controlled cortical impactor device designed by our laboratory in collaboration with the University of Georgia Instrument Design and Fabrication Shop (Athens, GA). Impactor design was modeled after the design of Manley and associates.[45] Briefly, the impactor is composed of a small-bore, double-acting, pneumatic cylinder with a piston that is mounted to an adjustable frame. A 15-mm impactor tip with beveled edges is attached to the lower end of a threaded rod. The upper end of the rod is attached to the transducer core of a linear voltage differential transducer (LVDT). Fine-tuning the flow of pressurized gas to the pneumatic piston controls the velocity of the impactor. Velocity is calculated from the time/displacement curve measured by the LVDT and recorded by the computerized data acquisition system DAQ Central. In addition, a CLICK® Series Programmable Logic Controller (PLC) is used to regulate the dwell time of the impactor rod.

After surgical preparation, the piglet was transferred to the CCI device mounted on a large animal stereotaxic frame, secured in place using ear bars and straps, and the impactor tip was positioned over the craniectomy site. For this initial study, we chose to assess the effects of injury severity by manipulating either the velocity or depth of depression, or both. Piglets were divided into four groups defined by the impact parameters in which TBI was induced: 2 m/sec impact velocity with 6 mm depth of depression ($n=4$), 4 m/sec impact velocity with 6 mm depth of depression ($n=4$), 4 m/sec impact velocity with 12 mm depth of depression ($n=4$), and 4 m/sec impact velocity with 15 mm depth of depression ($n=4$). The dwell time was held constant at 400 msec for all animals.

After injury, the surgical site was flushed with sterile saline, and the skin was re-apposed with surgical staples. Banamine® (1.1 mg/kg

intramuscular [IM]) and butorphanol (0.2 mg/kg IM) was administered post-operatively for pain management, and ceftiofur sodium (Naxcel®; 4 mg/kg IM) was administered as an antibiotic. Anesthesia was discontinued, and piglets were allowed to recover until ambulatory before being returned to their home pens. Piglets were monitored every 8 h for the next 24 h, and any abnormal neurological behaviors were recorded.

Gait analysis

One week before the surgical procedure, piglets were placed individually in a semi-circular gait analysis track in a separate climate-controlled room for gait track familiarization and training. Piglets were familiarized to the testing room and trained to move down the track for three days before data collection. After training, each piglet was video recorded on three separate days before TBI operation to obtain pre-TBI gait measurements. Piglets were also evaluated on days one, three, and seven post-TBI.

Gait analysis was performed as described previously.[47] Briefly, two high speed GigEye Ethernet Cameras (IDS Imaging Development Systems, Obersulm, Germany) set to capture footage (70 frames per second) of each side of the pig in profile view were synchronized through an IDS computer driver. Piglets were recorded as they walked through the straight portion of the semi-circular track, where they were video recorded as they moved perpendicular to the two synchronized cameras recording each side of the piglet. Piglets were moved through the track until five usable repetitions were obtained. Video data were analyzed using Kinovea software (Kinovea open source project, www.kinovea.org) by an unblinded investigator to obtain swing time, stance time, stride velocity, and two-limb versus three-limb support measurements.

To ensure unbiased analysis, the research team developed specific, uniform criteria to define key metrics, components, and points for each analyzed gait parameter. Once defined, a training set of data was analyzed by at least two researchers, and the results were then evaluated to ensure that there was agreement between the researchers on the developed criteria, the overall approach, and the correctness of the result. This unbiased analysis approach was then uniformly applied to the gait data.

Lesion size assessment

One week post-TBI, piglets were deeply anesthetized using 5% vaporized isoflurane in oxygen and euthanized via CO_2 inhalation. After euthanasia, brains were removed and fixed in 10% buffered formalin for lesion size measurement and histology.

For lesion size measurement, four serial coronal sections measuring 5 mm each were obtained from the lesion site, paraffin embedded, sectioned, and stained with cresyl violet and luxol fast blue. Slides were scanned using an Aperio Digital Pathology Slide Scanner (Leica Biosystems). The lesion area and the area of the contralateral hemisphere was measured by a blinded investigator using ImageJ software,[48] and lesion size was expressed as a percentage of the contralateral hemisphere.

Histology

Representative sections from each animal were collected, processed routinely, embedded in paraffin, sectioned at 4 mm, and stained with hematoxylin and eosin to evaluate the lesion microscopically. Additional sections were stained by immunohistochemistry for glial fibrillary acidic protein (GFAP; 1:4000; mouse; Biogenex), Olig2 (1:400; rabbit; Genetex), and neuronal nuclei (NeuN; 1:500, guinea pig, Millipore) as described previously.[49] Heat induced antigen retrieval was performed for GFAP, Olig2, and NeuN using citrate buffer at pH6 (DAKO). Detection was performed using biotinylated anti-mouse (GFAP; Biocare), anti-guinea pig (NeuN; Biogenex), or anti-rabbit (Olig2; Biocare) antibodies, and a streptavidin label (4plus Streptavidin HRP or AP label; Biocare), and 3,3'-Diaminobenzidine (DAB) as the chromogen (DAKO). All sections were counterstained with hematoxylin.

For quantification, a perilesional region of interest was defined, which included dorsal and dorsolateral gyri (cingulate, marginal, suprasylvian and sylvian, and/or ectosylvian), and five fields were imaged per section using an Olympus BX41 light microscope (Center Valley, PA). Utilizing ImagePro Plus software, the percentage of cells positive for NeuN and Olig2 were counted manually and GFAP was quantified by relative threshold value by a blinded investigator.

Statistics

Immunohistochemistry data were analyzed with SigmaPlot version 12.5 (San Jose, CA), and statistical differences between the lesion site and contralateral hemisphere within each TBI group were determined by a *t* test. Lesion size and gait data were analyzed with SAS version 9.3 (Cary, NC), and statistical significances between groups were determined by one-way analysis of variance followed by *post hoc* Tukey pair-wise comparisons. For all data, comparisons where p values were ≤ 0.05 were considered to be significantly different.

Results

Brain lesion severity increases as depth of depression increases

Lesion size as a percentage of the contralateral hemisphere was calculated to determine the extent of brain injury as impact velocity and depth of depression was increased. Piglets in the 2 m/sec; 6 mm; and 4 m/sec; 6 mm groups (velocity and depth, respectively) had minor brain lesions, and there was no significant difference in lesion size between the two groups ($1.79\% \pm 0.45\%$ vs. $1.49\% \pm 0.47\%$, respectively, Fig. 1A, 1B, 1E).

When depth of depression was increased to 12 mm, however, there was a significant ($p < 0.001$) increase in lesion size compared with both the 2 m/sec; 6 mm; and 4 m/sec; 6 mm groups ($11.03\% \pm 0.67\%$ vs. $1.79\% \pm 0.45\%$ and $1.49\% \pm 0.47\%$, respectively, Fig. 1C, 1E). Further, when depth of depression was increased to 15 mm while maintaining the impact velocity at 4 m/sec, lesion size was also significantly ($p < 0.001$) increased compared with the 2 m/sec; 6 mm; and 4 m/sec; 6 mm groups ($11.16\% \pm 1.40\%$ vs. $1.79\% \pm 0.45\%$ and $1.49\% \pm 0.47\%$, respectively, Fig. 1D, 1E). Taken together, these results indicate that the brain lesion increased in severity as depth of depression was increased from 6 mm to 12 mm and 15 mm.

Histopathology reveals correlative increase in lesion size in response to injury severity

In the 2 m/sec; 6 mm group, microscopic changes were subtle. Tips of gyri (marginal, suprasylvian, and/or sylvian) at the lesion site had increased cellularity (gliosis) in both cortex and white matter and rare shrunken necrotic cortical neurons (Fig. 2A). Mild fibrosis of the leptomeninges overlying the lesion site was present. Immunohistochemistry for GFAP revealed mild multifocal astrocytosis/astrogliosis in the involved cortex and underlying white matter (Fig. 3A), but no subjective changes in oligodendrocytes were present on Olig2 staining (Fig. 4I).

The 4 m/sec; 6 mm group had more extensive changes, although similar to the 2 m/sec; 6 mm group in that changes were primarily at the tips of gyri (marginal, suprasylvian, and sylvian) at the lesion

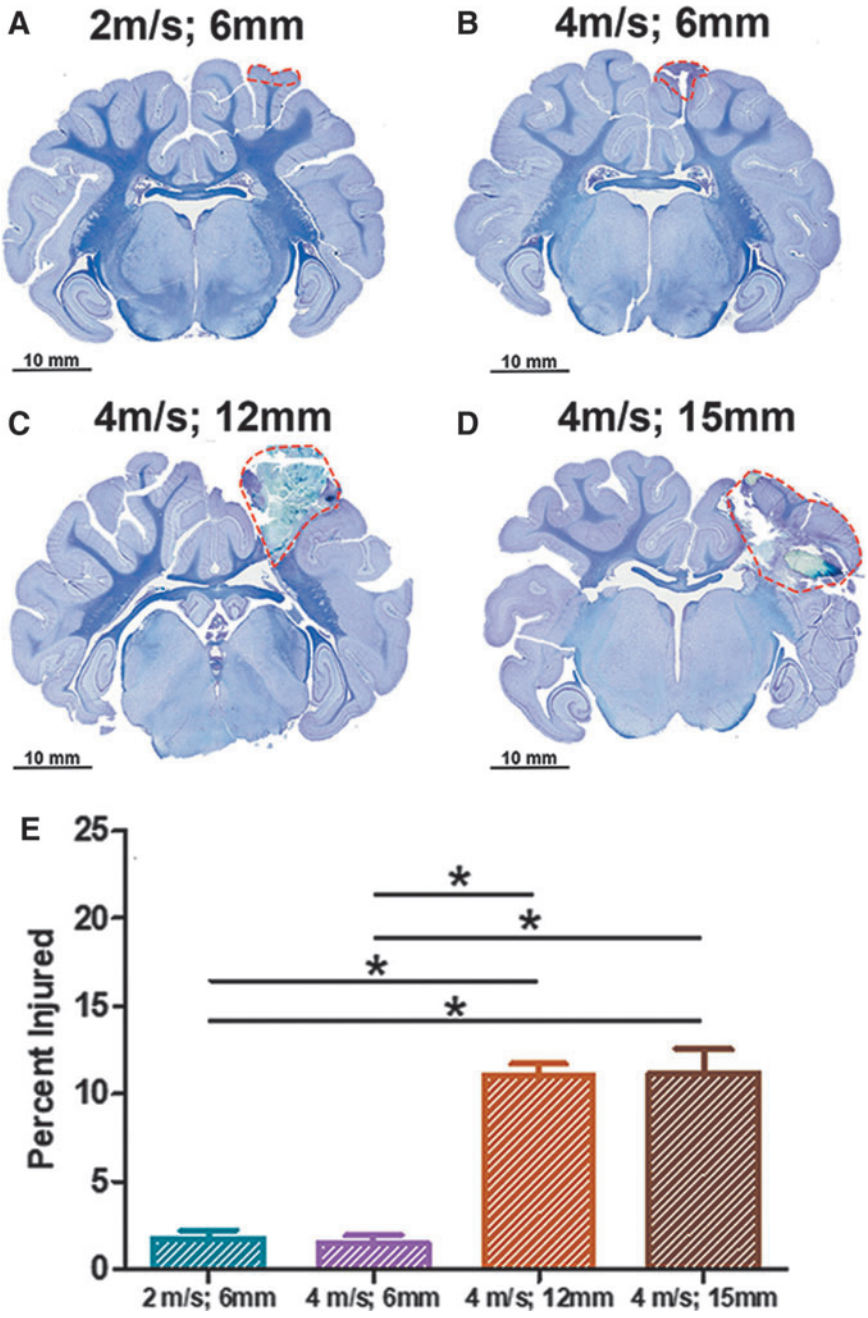

FIG. 1. Brain lesion severity increases as depth of depression increases. Brain sections of piglets impacted at 2 m/sec; 6 mm (**A**), 4 m/sec; 6 mm (**B**), 4 m/sec; 12 mm (**C**), and 4 m/sec; 15 mm (**D**) were stained with cresyl violet and luxol fast blue for lesion size measurement (lesion outlined by red dotted line). Piglets in all groups demonstrated measurable brain lesion; however, there was no significant difference in lesion size between the 2 m/sec; 6 mm (A, **E**) and the 4 m/sec; 6 mm (B, E) groups. When depth of depression was increased to 12 mm (C) and 15 mm (D), there was a significant increase in lesion size compared with the 2 m/sec; 6 mm and 4 m/sec; 6 mm groups (E) . * indicates significance between groups ($p < 0.001$). Color image is available online at www.liebertpub.com/neu

site (Fig. 2B). This was characterized by more extensive neuronal necrosis and loss, reactive vessels, sometimes with mild perivascular cuffing by lymphocytes and plasma cells, and hypercellularity of both cortex and white matter in the involved area because of gliosis and infiltrating gitter cells. Unlike the 2 m/sec; 6 mm group, some animals had shallow tracks filled with hemorrhage and/or gitter cells in the area of impact. In addition, there were hemosiderin laden macrophages, hemorrhage, mild perivascular cuffing by lymphocytes and plasma cells, and fibrosis in the overlying leptomeninges. By immunohistochemistry, there was increased staining for GFAP around the lesion site (Fig. 3B).

In the 4 m/sec; 12 mm group, changes were more severe and were present in all the dorsolateral gyri (marginal, suprasylvian, and sylvian) and sometimes the cingulate gyrus (Fig. 2C). The immediate area of impact was disrupted deep into the white matter and mostly replaced with hemorrhage and macrophages containing

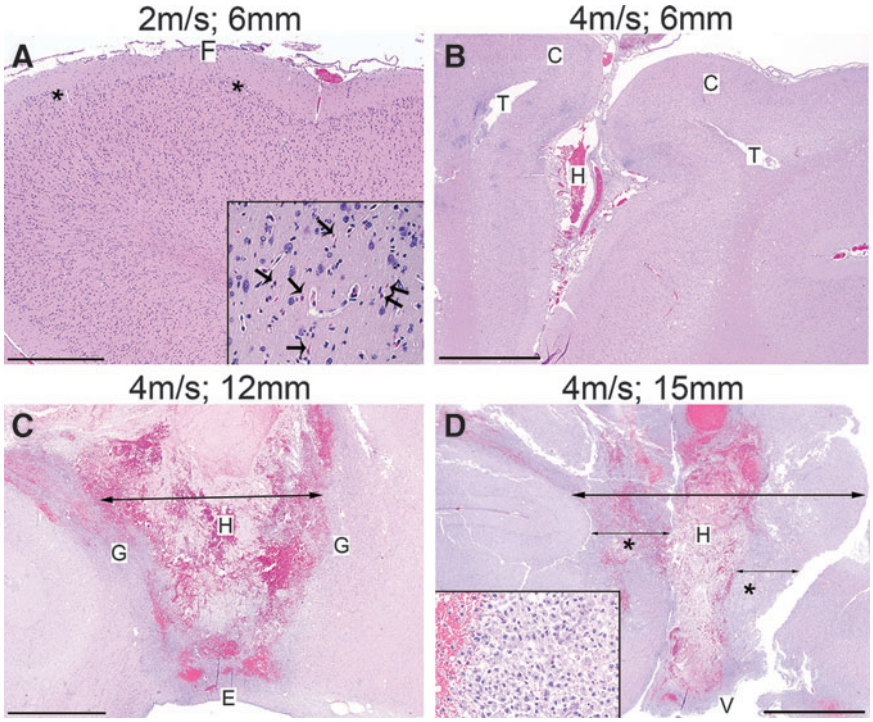

FIG. 2. Histopathology reveals correlative increase in lesion size in response to injury severity. Hematoxylin and eosin staining of piglets impacted at 2 m/sec; 6 mm **(A)**, 4 m/sec; 6 mm **(B)**, 4 m/sec; 12 mm **(C)**, and 4 m/sec; 15 mm **(D)**. For 2 m/sec; 6 mm, impact lesion is subtle and corresponds to focus of increased glial fibrillary acidic protein staining in Figure 3A at arrow. Note area of decreased cellularity in the cortex under the slightly fibrotic leptomeninges (**F**) and roughly between the *s. Decreased cellularity is because of shrunken eosinophilic necrotic neurons (see inset). Inset: Higher magnification showing necrotic neurons (arrows mark some but not all) in area of decreased cellularity (A). For 4 m/sec; 6 mm, impact lesion is more extensive spanning multiple gyri but still relatively superficial. Note the expansion and severe cellularity because of gliosis of the cortex (C) of two gyri. There are also two tracts (**T**) of tissue loss that contain small numbers of gitter cells as indicated by the increase in cellularity. Hemorrhage (**H**) is present in the leptomeninges in the sulcus between the gyri (B). For 4 m/sec; 12 mm, impact lesion is severe and extends deep into the cerebrum almost through the ependyma lining the lateral ventricle (**E**). The large tract (delineated by double headed arrow) is filled with necrotic debris and hemorrhage (**H**). The surrounding neuroparenchyma is densely cellular because of gliosis (**G**) (C). For 4 m/sec; 15 mm, impact lesion is severe and extends deep into the cerebrum disrupting the ependymal and into the ventricle (**V**). The large tract (delinated by thicker double headed arrow) is filled with necrotic debris and hemorrhage (H) surrounded by a thick layer of infiltrating gitter cells (*s with thinner double headed arrows denoting thickness). Inset: Higher magnification showing infiltrating gitter cells at *s (D). Scale bars: A, 1 mm; B–D, 2 mm. Insets taken at 400X. Color image is available online at www.liebertpub.com/neu

hemosiderin. Surrounding the impact tract, adjacent cortex and white matter was hypercellular and the white matter, down to the lateral ventricle, had extensive degenerative changes consisting of axonal and myelin degeneration. The overlying leptomeninges were thickened by hemorrhage and an infiltration of macrophages, lymphocytes, neutrophils, and fibroblasts. There was a diffuse increase in staining for GFAP (astrocytosis/astrogliosis) surrounding the impact tract (Fig. 3C), but numbers of cells staining for Olig2 did not appear increased (Fig. 4I).

The 4 m/sec; 15 mm group had the most severe changes also involving the dorsolateral gyri (marginal, suprasylvian, and sylvian) and the cingulate gyrus (Fig. 2D). The lesion site was characterized by a large, deep tract of tissue necrosis and loss, often extending to the lateral ventricle and disrupting the ependymal lining, which was filled with hemorrhage and gitter cells. The tract was immediately surrounded by hemosiderin/hematoidin-laden gitter cells and a layer of gliosis with reactive vessels. Severe gliosis extended into the surrounding gyri and white matter, and the white matter had degenerative changes consisting of swollen axons and myelin degeneration. The overlying meninges were thickened by hemorrhage, infiltration of hemosiderin-laden macrophages, lymphocytes, plasma cells, and fibrosis. In one animal, the contralateral marginal gyrus had a large deep tract that extended to the ventricle and was filled with hemorrhage. Surrounding the impact tract, there was severe, diffuse staining for GFAP (astrocytosis/astrogliosis, Fig. 3D) and increased numbers of Olig2 stained cells in the white matter (Fig. 4I).

Immunohistochemistry reveals correlative loss of neurons and increased gliosis in response to injury severity

Immunohistochemical staining was performed on the perilesional region to assess changes in the number of neurons, astrocytes, and oligodendrocytes as a result of increasing TBI severity. A similar anatomical region on the contralateral hemisphere was utilized as the control to account for individual variability of basal neural cell numbers. First, staining for the neuron marker NeuN was used to quantify the number of perilesional mature neurons and the contralateral side. In the 2 m/sec; 6 mm group, the perilesion site was composed of 37.76% ± 3.58% NeuN+ cells compared with 45.37% ± 2.69% NeuN+ cells on the contralateral hemisphere,

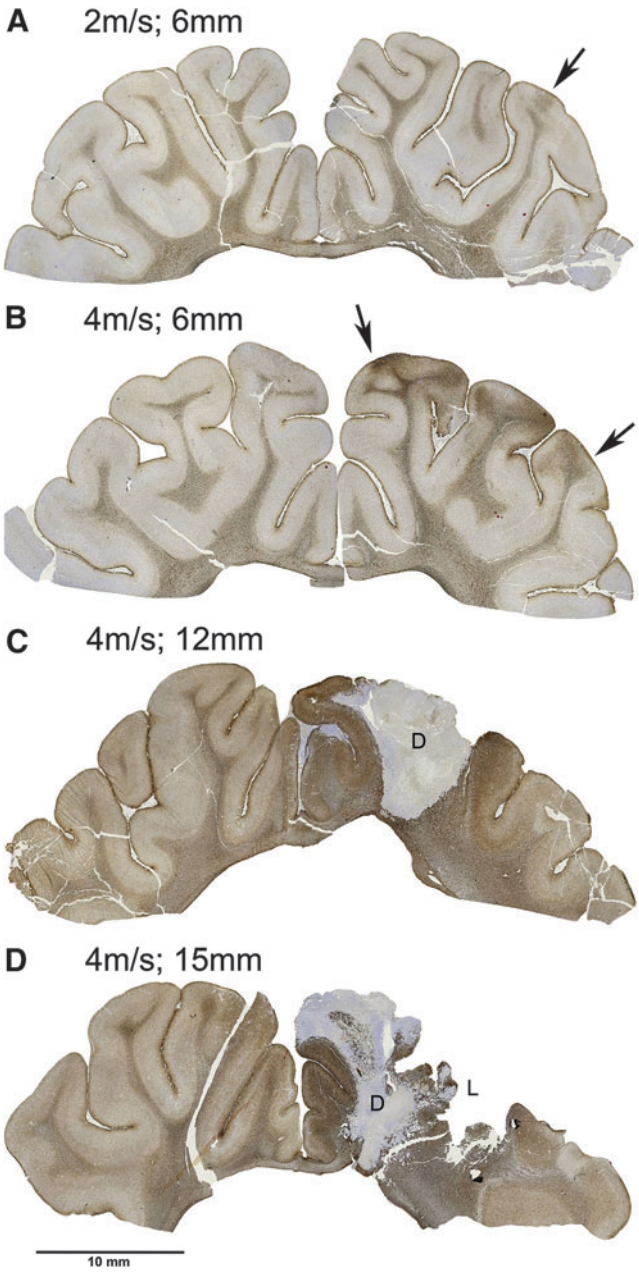

FIG. 3. Traumatic brain injury severity corresponds to increased astrocytosis and astrogliosis. Staining of glial fibrillary acidic protein (GFAP)+ reactive astrocytes in coronal sections of piglets impacted at 2 m/sec; 6 mm **(A)**, 4 m/sec; 6 mm **(B)**, 4 m/sec; 12 mm **(C)**, and 4 m/sec; 15 mm **(D)**. For 2 m/sec; 6 mm, the cerebral cortex at the tip of one dorsolateral gyrus has a small focal area of mildly increased staining for GFAP at the lesion site, (arrow, A). For 4 m/sec; 6 mm, the cerebral cortex at the tips of several dorsolateral gyri (marginal, suprasylvian, sylvian) has more extensive and moderately intense staining for GFAP at the lesion site (between arrows, B). For 4 m/sec; 12 mm, there is a large nonstained area of neuroparenchymal damage (D) at the lesion site that is surrounded by marked intense staining for GFAP of both cortical and white matter of the surrounding gyri, including the cingulate gyrus (C). For 4 m/sec; 15 mm, there is an extensive area of neuroparenchymal damage and loss (D and L, respectively) at the lesion site with markedly intense staining for GFAP in the surrounding cortical and white matter (D). Scale bar is 10 mm. Color image is available online at www.liebertpub.com/neu

indicating a decrease in NeuN+ cells around the lesion site, although not statistically significant (Fig. 4C).

The disparity of percent NeuN+ cells between the perilesion site and contralateral hemispheres became more pronounced when impact velocity was increased to 4 m/sec and further when depth of depression was increased. In the 4 m/sec; 6 mm group, there was a significant ($p < 0.01$) decrease in NeuN+ cells in the perilesion site compared with the corresponding contralateral side (32.28% ± 1.59% vs. 42.05% ± 1.95%, Fig. 4C). There was also a significant ($p < 0.005$) reduction in NeuN+ cells at the perilesion site compared with the contralateral hemisphere in the 4 m/sec; 12 mm group (29.34% ± 3.51% vs. 46.41% ± 1.62%, Fig. 4A–4C). Last, decreases in NeuN reactivity at the perilesion site was evident in the 4 m/sec; 15 mm group where there were only 29.03% ± 4.69% NeuN+ cells in contrast to 43.75% ± 1.35% NeuN+ cells on the contralateral side ($p < 0.05$, Fig. 4C). Taken together, there was a decrease in percentage of mature neurons around the lesion site as velocity and depth of depression was increased.

The dynamic changes in astrocyte numbers at the perilesion site was determined by staining for GFAP and comparing with the corresponding area on the contralateral hemisphere. A similar pattern observed for NeuN reactivity emerged for GFAP in the mildest, 2 m/sec; 6 mm group; a minimal increase in GFAP reactivity was present at the perilesion site and was comparable to the contralateral side (threshold value 1079.80 ± 454.00 vs. 1012.45 ± 359.38, Fig. 4F).

As injury severity increased, however, the disparity between GFAP reactivity at the perilesion site compared with the contralateral side became more distinct. The 4 m/sec; 6 mm group had a significant ($p < 0.05$) increase in GFAP reactivity at the perilesion site compared with the same anatomical region on the contralateral hemisphere (threshold value 1530.55 ± 224.28 vs. 690.65 ± 102.32, Fig. 4F). The 4 m/sec; 12 mm group also had a significant ($p < 0.01$) upregulation of GFAP around the lesion site compared with the contralateral side (threshold value 1592.1 ± 177.51 vs. 803.85 ± 63.81, Fig. 4E, 4F). Last, the 4 m/sec; 15 mm group also demonstrated a significant difference ($p < 0.05$) between the ipsilateral and the contralateral sides (1840.45 ± 329.72 vs. 989.50 ± 105.75, Fig. 4F). Therefore, activation of astrocytes, and thus astrogliosis/astrocytosis, became more pronounced as CCI parameters increased.

Last, we quantified the number of oligodendrocytes around the lesion site compared with the contralateral side utilizing staining for Olig2, which labels both mature oligodendrocytes and oligodendrocyte precursor cells. There was no significant difference in Olig2 positive cells around the lesion site compared with the contralateral side in the 2 m/sec; 6 mm group (29.64% ± 6.54% vs. 26.1% ± 1.80%, Fig. 4I), the 4 m/sec; 12 mm group (29.14% ± 3.98% vs. 35.16% ± 4.49%, Fig. 4G–4I), or the 4 m/sec; 15 mm group (26.17% ± 2.38% vs. 33.14% ± 6.51%, Fig. 4G). The 4 m/sec; 6 mm group, however, demonstrated a significant ($p < 0.05$) reduction in Olig2+ cells at the lesion site compared with the contralateral hemisphere (22.86% ± 3.31% vs. 34.39% ± 2.31%, Fig. 4I). Thus significant changes in oligodendrocyte numbers did not strongly correlate to increases in injury severity.

Motor deficits become more pronounced with increasing impact velocity and depth of depression

To measure potential deficits in motor function, gait analysis was performed first before TBI to serve as a baseline and then one, three, and seven days post-TBI. Changes in swing time, stance

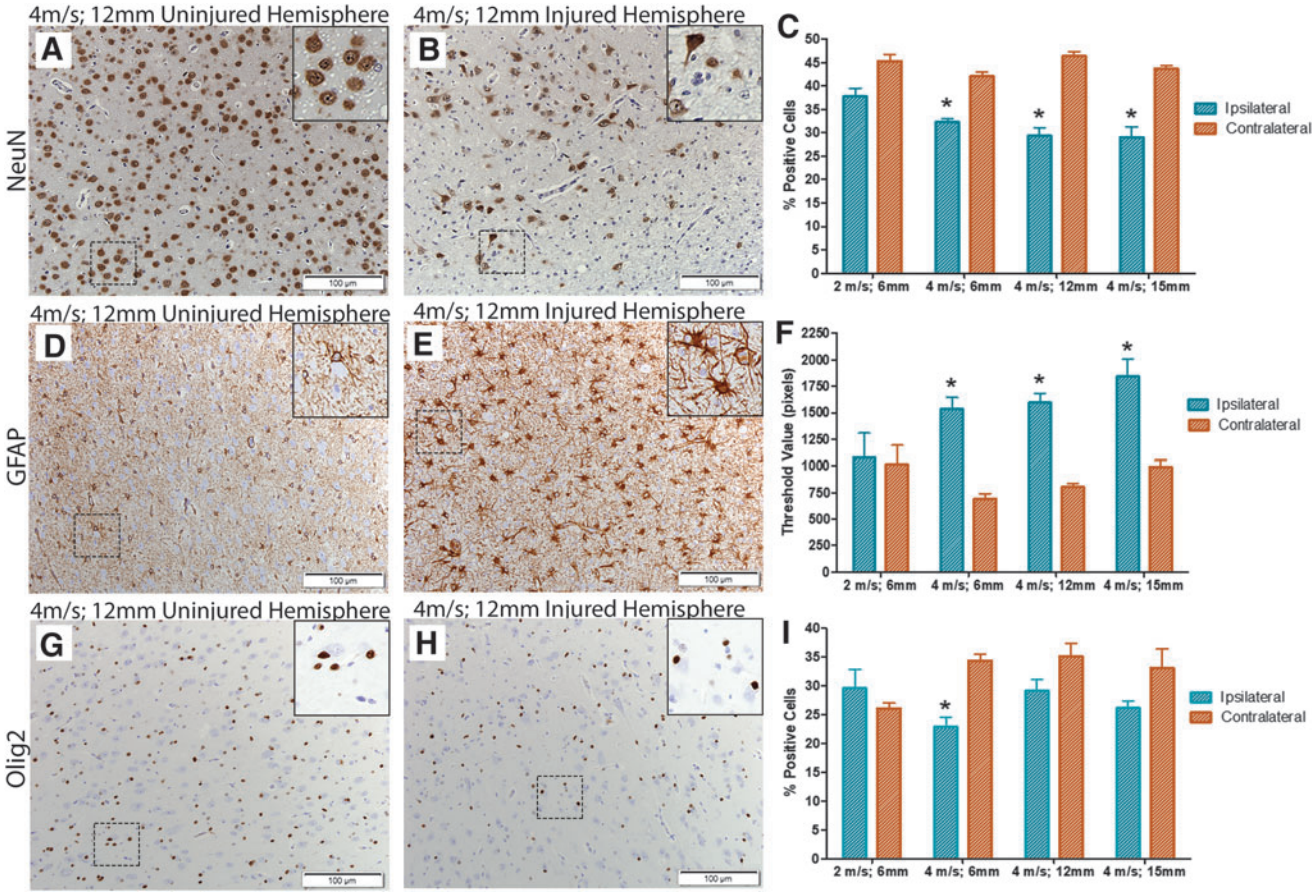

FIG. 4. Traumatic brain injury (TBI) severity corresponds to loss of NeuN+ neurons and upregulation of glial fibrillary acidic protein (GFAP)+ astrocytes. Representative images of NeuN expression in 4 m/sec; 12 mm uninjured (**A**) and injured (**B**) hemispheres. NeuN expression was significantly reduced in the ipsilateral hemisphere compared with the contralateral hemisphere in the 4 m/sec; 6 mm, 4 m/sec; 12 mm; and 4 m/sec; 15 mm groups seven days post-TBI (**C**). Representative image of GFAP expression in 4 m/sec; 12 mm uninjured (**D**) and injured (**E**) hemispheres. GFAP expression was significantly increased in the ipsilateral hemisphere compared with the contralateral hemisphere in the 4 m/sec; 6 mm, 4 m/sec; 12 mm; and 4 m/sec, 15 mm groups seven days post-TBI (**F**). Representative image of Olig2 expression in 4 m/sec; 12 mm uninjured (**G**) and injured (**H**) hemispheres. Olig2 expression was unchanged in the ipsilateral hemisphere compared with the contralateral hemisphere for all groups seven days post-TBI (*I*). Boxes with dotted lines correspond to insets in the top right corner of each image. * indicates significant difference compared to contralateral side at $p < 0.05$. Color image is available online at www.liebertpub.com/neu

time, stride velocity, two-limb support, and three-limb support were assessed as a function of increasing impact velocity and depth of depression using Kinovea gait analysis software (Fig. 5A). Stance percent of each limb, represented as the percentage of stride duration with the limb in ground contact, was assessed pre- and post-TBI to determine whether injury resulted in an increased need for ground support. For both the 2 m/sec; 6 mm and 4 m/sec; 6 mm groups, animals spent approximately half their stride duration in stance phase pre-TBI (47.6% ± 1.7% and 47.18% ± 0.63%, Fig. 5B).

Stance percent remained unchanged at all time points after TBI, indicating a consistent stance:swing ratio throughout the study. The 4 m/sec; 12 mm group, however, demonstrated a significant ($p < 0.001$) increase in percent stance time and spent almost 20% more time in stance phase one day post-TBI compared with pre-TBI (62.07% ± 2.93% vs. 43.04% ± 1.1%, Fig. 5B). A significant ($p < 0.01$) increase in percent stance time persisted through both three and seven days post-TBI (61.62% ± 1.58% and 56.07% ± 3.22%, Fig. 5B). Further, the 4 m/sec, 15 mm group also displayed significant ($p < 0.0001$) increases in percent stance time and spent almost 18% more time in stance phase one day post-TBI compared with pre-TBI (62.765% ± 0.40% vs. 45.25% ± 0.65%, Fig. 5B). Animals maintained a significantly ($p < 0.001$) increased percent stance time at both three and seven days post-TBI (58.59% ± 2.10% and 59.36% ± 1.70%, Fig. 5B). Taken together, these data suggest that increasing both velocity and depth of depression to 12 or 15 mm results in a shift in the stance:swing ratio such that animals spend more time in stance phase during one stride cycle.

Stride velocity, or the time to complete one stride cycle, was used as a measure to detect changes in rate of movement after TBI. Stride velocity remained largely unaffected through all post-TBI time points for both the 2 m/sec; 6 mm and 4 m/sec; 6 mm groups compared with pre-TBI assessment (1.76 m/sec ± 0.11 m/sec and 1.58 m/sec ± 0.04 m/sec, Fig. 5C). Stride velocity was significantly ($p < 0.001$) slower, however, for the 4 m/sec; 12 mm group one day post-TBI compared with pre-TBI (0.68 m/sec ± 0.14 m/sec vs. 1.77 m/sec ± 0.10 m/sec), and remained slower both three and seven days post-TBI (1.05 m/sec ± 0.36 m/sec, 1.02 m/sec ± 0.24 m/sec), although day three and seven results did not reach significance

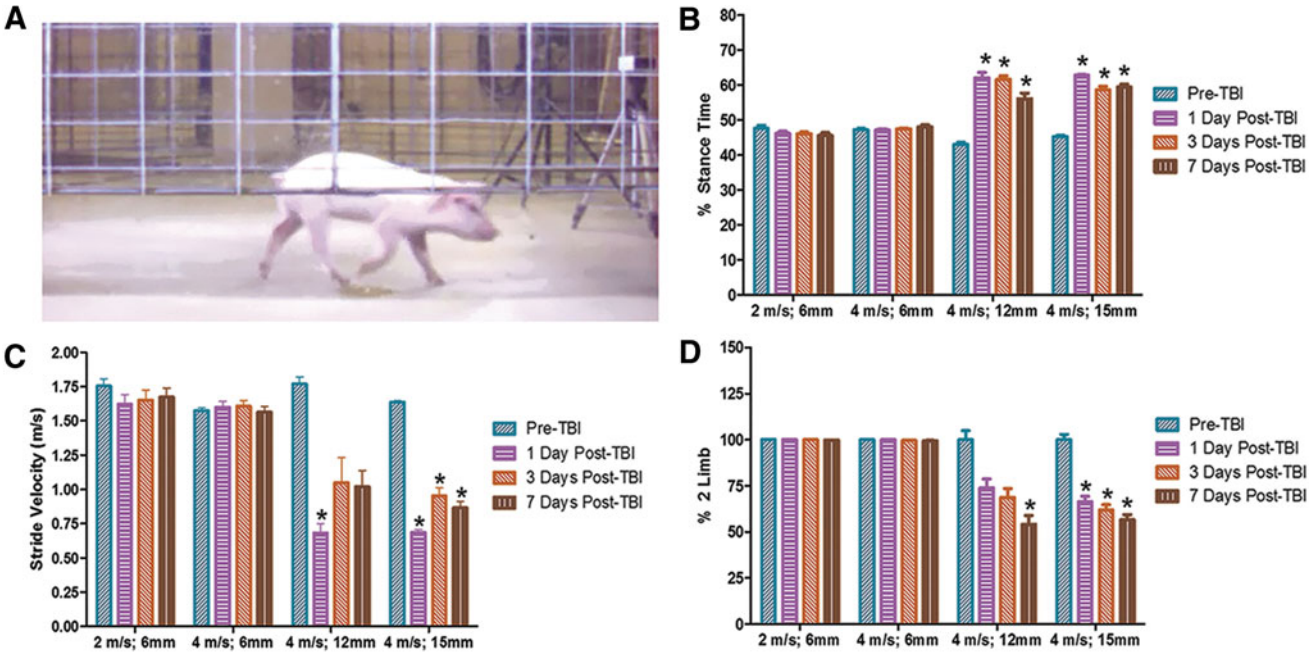

FIG. 5. Piglets that received a traumatic brain injury (TBI) with a depth of depression of 12 mm or 15 mm demonstrate significant motor deficits that persisted seven days post-TBI. Gait videos were analyzed in Kinovea software frame by frame for changes in stance time, swing time, stride velocity, two-limb support, and three-limb support **(A)**. Piglets that received a TBI with a 4 m/sec impact velocity and either 12 mm or 15 mm depth of depression demonstrate a significant increase in stance time at one, three, and seven days post-TBI **(B)**. Piglets that received a TBI with a 12 mm depth of depression showed a significant decrease in stride velocity one day post-TBI, and piglets that received a TBI with a 15 mm depth of depression showed a significant decrease in stride velocity one, three, and seven days post-TBI **(C)**. Piglets that received a TBI with a 12 mm depth of depression demonstrated a significant decrease in two-limb support at seven days post-TBI, while piglets that received a TBI with a 15 mm TBI demonstrated a significant decrease in two-limb support at one, three, and seven days post-TBI **(D)**. No significant changes in motor function were observed for any gait parameters in piglets that received a TBI with a depth of depression of 6 mm at either 2 m/sec or 4 m/sec velocity. The % stance time is represented as the percent of time spent in stance phase of the stride compared with the swing phase of the stride, and % two-limb support is represented as the percent of time spent in two-limb support compared with three-limb support during a full stride cycle. * indicates significant difference compared with pre-TBI at $p < 0.05$. Color image is available online at www.liebertpub.com/neu

(Fig. 5C). Stride velocity was significantly ($p < 0.001$) slower, however, for the 4 m/sec; 15 mm group one, three, and seven days post-TBI (0.69 m/sec ± 0.05 m/sec, 0.95 m/sec ± 0.12 m/sec, and 0.87 m/sec ± 0.01 m/sec, respectively) compared with pre-TBI (1.64 m/sec ± 0.02 m/sec, Fig. 5C). These results indicate that stride velocity was reduced as a result of increasing TBI severity.

Limb support was measured as time spent with either two limbs in ground contact (two-limb support) or three limbs in ground contact (three-limb support). A decrease in percent of time in two-limb support corresponds to an increase in percent of time in three-limb support and suggests a decrease in balance and need for additional support post-TBI. Percent of time spent in two-limb support remained relatively unchanged for both the 2 m/sec; 6 mm and 4 m/sec; 6 mm groups after TBI for all time points compared with pre-TBI (100% ± 0.11%, 100% ± 0.30%, Fig. 5D). For the 4 m/sec; 12 mm group, percent time spent in two-limb support decreased one and three days post-TBI compared with pre-TBI (73.79% ± 9.79% and 68.65% ± 9.79% vs. 100% ± 9.79%, respectively), although these results did not reach significance. Percent two-limb support, however, significantly ($p < 0.05$) decreased by almost 46% seven days post-TBI compared with pre-TBI (54.04% ± 9.79% vs. 100% ± 9.79%, Fig. 5D).

The 4 m/sec, 15 mm group's percent time spent in two-limb support significantly ($p < 0.001$) decreased by almost 34% one day post-TBI compared with pre-TBI (66.39% ± 5.82% vs. 100% ± 5.82%, Fig. 5D). Interestingly, time spent in two-limb support continued to decrease over time, as opposed to stance time and stride velocity where small increments of improvement were noted at three and seven days post-TBI. Percent two-limb support significantly decreased by almost 38% three days post-TBI and by almost 54% seven days post-TBI compared with pre-TBI (61.86 ± 5.82% and 46.51 ± 5.82% vs. 100% ± 5.82% respectively, $p < 0.05$, Fig. 5D). Taken together, these data suggest that uninjured animals and injured animals with a mild TBI typically relied on only two-limb support, but that increasing velocity and depth of depression resulted in a shift from two-limb only support to a combination of two- and three-limb support.

Discussion

In this study, we characterize a graded piglet TBI model generated using an open skull CCI approach in which the histopathological and functional responses to injury increase as a function of cortical impact speed and depth of depression. Increasing the velocity and depth of depression of impact contributed to significant increases in lesion volume seven days post-TBI. Affected regions demonstrated macro- and microcellular changes in the brain that ranged from mild damage, mostly at the cortical surface and mild astrocytosis/astrogliosis, to severe damage with large tracts of necrosis, neuroparenchymal loss in gray and white matter, and intense astrocytosis/astrogliosis. Most importantly, functional changes were observed that corresponded with TBI severity.

Gait analysis revealed progressive motor function deficits in stance percent, stride velocity, and limb support as CCI parameters increased. These changes are summarized in Table 1. These results suggest that this piglet TBI model may be an ideal model for use in future studies aimed at further elucidating the complexities of TBI pathophysiology, time course, and functional responses, and may have greater predictive power pertaining to efficacy of potential therapeutics.

CCI was selected to generate a TBI because this approach has proven to be reliable and repeatable in both rodent and pig models.[50] The surgical approach is relatively quick and takes less than 1 h from initial skin incision to final closure. This procedure resulted in no deaths, even in our most severe group, despite all pigs exhibiting significant neurological impairments. We developed our CCI device after the design of Manley and associates[45] using a gas driven pneumatic piston to allow for the precise control of the impact parameters, thus giving us the ability to manipulate injury severity.

It has been well established that manipulation of velocity, depth of depression, and dwell time either individually or in combination can affect injury severity. We took several factors into account when selecting each combination of impact parameters that would best produce features of human TBI. First, a dwell time of 400 msec was selected for all groups, similar to previous reports.[43–45,51] Duhaime and colleagues[43] developed a piglet TBI model at three different maturational stages at five days, one month, and four months of age, which correspond to infants, toddlers, and adolescents, respectively. Depth of depression for five-day, one-month, and four-month old animals varied from 5 mm, 6 mm, and 7 mm, respectively, and velocity was held constant at 1.7 m/sec for all maturation stages.

Similarly, in this study, we used one month old piglets and selected a velocity of 2 m/sec and a depth of depression of 6 mm as our initial CCI parameters to achieve a small focal contusion. To achieve a more moderate to severe TBI, we increased velocity to 4 m/sec, similar to a report by Jin and coworkers.[52] To achieve a more severe injury, we held velocity constant at 4 m/sec and increased depth of depression to 12 mm and 15 mm. While previous CCI studies in similarly aged piglets have not reported a depth of depression greater than 6 mm, depth of depressions of 12 mm and 15 mm have been reported in adult pig CCI studies and were selected in an effort to achieve both histopathological and functional deficits.[45,46,53]

In the present study, we assessed changes in lesion size to determine the extent of tissue damage as a result of increasing TBI severity. Human MRI studies have found that lesion volume is a critical predictor of outcome after TBI and that lesion volume directly correlates with long-term functional outcomes using multiple clinical scales.[54,55] In addition, lesion size, characterized by the number of affected brain regions, correlates with the extent of motor deficits and affects the time of recovery.[7] We found a positive relationship between lesion size and CCI parameters in that lesion size dramatically enlarged as depth of depression increased from 6 mm to 12 mm and 15 mm.

It can be noted that in this study, similar to humans, we observed a clear correlation between lesion size and motor deficits. The 4 m/sec; 12 mm and 4 m/sec; 15 mm groups with the largest lesion volumes exhibited the greatest impairments in gait. These results highlight the functional consequences of increasing TBI severity and support clinical TBI findings that lesion size could serve as a predictive marker of motor function impairment.

In this report, we provide both a qualitative and quantitative assessment of histological changes across groups. Hematoxylin and eosin stained brain slices were reviewed by a board certified veterinary pathologist and assessed for specific pathological hallmarks of TBI commonly observed in humans.[56] Histological assessment revealed increasing damage with increasing velocity and depth of impact. Low velocity and depth of depression resulted in a small superficial cortical focus of subtle damage characterized by neuronal necrosis and reactive gliosis. As velocity increased, cortical damage and gliosis became more widespread, although still relatively superficial, with associated hemorrhage, necrosis, and

Table 1. Summary of Major Cellular, Tissue, and Functional Changes at Each Injury Severity

	2m/sec; 6 mm	*4m/sec; 6 mm*	*4m/sec; 12 mm*	*4m/sec; 15 mm*
Cellular	• Mild astrocytosis and astrogliosis at tips of gyri, cortex, and white matter	• Moderate astrocytosis and astrogliosis at tips of gyri, cortex, and white matter • Neuronal loss in the perilesion site • Limited shallow impact tracts with hemorrhage	• Severe astrocytosis and astrogliosis in impact tract, adjacent cortex, and white matter • Neuronal loss in the perilesion site • Hemorrhage in gyri and white matter • Axonal and myelin degeneration	• Severe astrocytosis and astrogliosis • Neuronal loss in the perilesion site • Hemorrhage of the meninges, impact tract, and ependymal lining • Swollen axons and myelin degeneration
Tissue	• Minor brain lesion (<2% of contralateral hemisphere)	• Minor brain lesion (<2% of contralateral hemisphere)	• Severe brain lesion (11% of contralateral hemisphere)	• Severe brain lesion (11% of contralateral hemisphere)
Functional	• No changes in stance time • No changes in stride velocity • No change in 2-limb support time	• No change in stance time • No changes in stride velocity • No change in 2-limb support time	• Increased percent stance time through 7 days post-TBI • Decreased stride velocity through 1 day post-TBI • Decreased 2-limb support beginning 7 days post-TBI	• Increased percent stance time through 7 days post-TBI • Decreased stride velocity through 7 days post-TBI • Decreased 2-limb support beginning 1 day post-TBI through 7 days post-TBI

Injury severity indicators (2 m/sec; 6 mm, 4 m/sec; 6 mm, 4 m/sec; 12 mm, 4 m/sec; 15 mm) represent the controlled cortical impact impact velocity and depth of depression, respectively.

vascular reaction, as well as underlying white matter changes. As the depth of depression increased, associated lesions became large tracts of necrosis, tissue loss, and hemorrhage extending deep into the cerebrum often down to the ventricle. These larger lesions were surrounded by a more intense gliosis and vascular reaction, and more severe white matter degeneration.

Similarly, increasing CCI severity in adult pigs has been shown to result in increased presence of vascular congestion and decreased loss of normal cytoarchitecture that corresponded with depth of depression.[45] In addition, TBI in the immature pig has revealed similar pathological features such as necrosis, hemorrhage, neuronal loss, and reactive gliosis at the site of injury.[43,57,58]

Histological changes have been quantitatively evaluated previously using a numerical scoring system that ranks the severity of specific pathological features of TBI.[44,51] Quantification of changes in neurons, astrocytes, and oligodendrocytes, the three major cell types of the brain, after TBI in a pig brain is lacking, however. Therefore, in the current study, immunohistological staining was performed with the well-established markers NeuN, GFAP, and Olig2 to assess the relative number of neurons, astrocytes, and oligodendrocytes, respectively, in the perilesion area one week post-TBI.

NeuN is a DNA-binding, neuron-specific protein expressed in post-mitotic neurons.[59] NeuN staining of human TBI-affected brain tissue has been shown to decrease at or near the site of injury as a result of neuronal cell death.[60] In addition, rodent TBI studies reveal similar loss of neurons in response to injury and have been found to be sensitive to injury severity.[19,61,62] In our piglet TBI model, based on NeuN staining, the percent of mature neurons was significantly reduced for all groups except for the most mild, 2 m/sec; 6 mm group, suggesting that neurons are sensitive to increasing TBI severity in this model.

GFAP, a cytoskeletal astrocytic marker, is well documented to measure astrocyte proliferation (astrocytosis) and hypertrophy (astrogliosis) after TBI.[63,64] Reactive astrocytes grow in size, proliferate, and migrate to the site of injury where they release neurotrophic factors, promoting tissue repair.[65] Astrocytosis and astrogliosis, however, can also contribute to glial scar formation, which can be detrimental to axonal regrowth and, ultimately, can contribute to neurodegeneration and the development of functional deficits.[66] GFAP expression is typically most highly upregulated at the site of the lesion and becomes less prominent in the perilesioned area in humans.[60,67] Graded injury in rodent CCI models have shown that GFAP expression corresponds with injury severity.[20] Globally, we observed substantial astrocytosis and astrogliosis at and near the site of the lesion for the 4 m/sec; 6 mm, 4 m/sec; 12 mm, and 4 m/sec; 15 mm groups and, in accordance, noted a significant upregulation of GFAP expression for these groups.

Last, Olig2, a basic helix loop helix (bHLH) transcription factor, is expressed in a number of different cell types including oligodendrocyte precursor cells and mature oligodendrocytes.[68] Oligodendrocytes are responsible for the myelination of axons. TBI in humans results in the death of mature oligodendrocytes followed by increases in oligodendrocyte precursor cells.[69] These dynamic changes may influence white matter function after TBI. Rodent TBI studies report similar changes in oligodendrocyte numbers in response to injury.[70,71] Interestingly, the present study only observed a decrease in Olig2+ oligodendrocytes in one TBI group.

Because Olig2 is expressed in both proliferating and mature oligodendrocytes, this result may be explained partially by initial mature oligodendrocyte death followed by proliferation of immature oligodendrocyte progenitors, resulting in minimal and transient changes in overall Olig2+ cell count. Indeed, Dent and associates[70] characterized a similar course of oligodendrocyte pathology in a rodent CCI model. Future studies may benefit from looking at changes in myelin basic protein to assess direct changes in white matter composition as a result of TBI.

Impairments in motor proficiency may develop in children who sustain a TBI. Several studies have evaluated motor deficits after TBI in children using quantitative gait analysis and found that children may exhibit deficits in spatiotemporal gait parameters.[7,18,72] Our group previously has developed a highly sensitive approach to assess changes in spatiotemporal gait parameters in a middle cerebral artery occlusion ischemic stroke pig model using high speed video cameras.[73] We present for the first time gait analysis performed in a piglet CCI model to assess impairments in motor function. We measured the response of stance percent, stride velocity, and limb support as a function of TBI severity. The 4 m/sec; 12 mm and 4 m/sec; 15 mm groups exhibited significant deficits in stance percent after TBI, similar to TBI-affected children.[74]

Increased overall stance percent may be explained by two reasons. First, the amount of time the pig spends in swing time may be reduced in an effort to hasten ground contact to begin the stance phase during which the pig is better able to stabilize its weight distribution. Second, limb weakness on the affected right side may limit the amount of propulsive forces needed to initiate and maintain the swing phase, resulting in a reduction of the time the hoof spends off the ground. Reduced stride velocity is one of the most common motor deficits observed as a result of moderate or severe TBI in children.[74,75] Stride velocity was significantly reduced for the 4 m/sec; 12 mm group one day post-TBI, and at all time points for the 4 m/sec; 15 mm group.

Similar to human studies, pigs were given the option to move at a self-selected pace. We observed that normal piglets' natural gait of choice is a two-beat gait with alternating diagonal limb support sequences. Post-TBI pigs that sustained a more severe injury, however, exhibited a shift toward a typical quadruped walking gait with alternating two- and three-limb support sequences. We found that there was a significant shift in two-limb support to three-limb support for the 4 m/sec; 12 mm group seven days post-TBI, and at all time points for the 4 m/sec; 15 mm group, which suggests that the pigs altered both their speed of travel and their gait support as a result of TBI.

Children who sustain a TBI may exhibit impairments in functional balance performance as a result of altered control of static and dynamic stability.[76,77] Changes in gait parameters such as velocity, step width, step length, and limb support after TBI have been found to reflect an individual's ability to maintain proper dynamic stability.[78,79] For example, decreases in velocity, increases in stance percent, and double limb support have been observed in individuals affected by TBI to better stabilize their gait and maintain balance.[79,80] Similarly, experimental studies in rodents observed comparable changes in gait as a result of TBI.[81,82]

The specific neural deficits that contribute to motor impairments in this study are unknown. In more moderately to severely injured pigs, we observed widespread necrosis, hemorrhage, loss of neurons and increased gliosis at the cortex, and evidence of white matter degeneration, which could disrupt the integration and processing of incoming sensory inputs from motor, proprioceptive, and/or vestibular systems into the appropriate motor outputs

needed to maintain balance.[79,83] Additional studies are needed to more closely examine the specific brain structures affected by TBI that contribute to motor function impairments observed in this pig model. Taken together, these findings indicate that injury severity influences functional outcomes and that, similar to children, impairments in balance and motor function develop in more moderately to severely affected pigs.

In this study, we developed and characterized a piglet CCI TBI model. The piglet has several key similarities to children in both neuroanatomy and brain development making it more translational than traditional rodent models. Manipulating CCI parameters resulted in a reproducible, graded injury with increasing lesion size. The lesion site increased from a small superficial focus of neuronal necrosis and gliosis in the mildest impact to a large deep tract of necrosis and tissue loss with marked astrogliosis/astocytosis and more extensive white matter changes in the more severe impacts. TBI produced motor impairments in gait that correlated with injury severity. This piglet TBI model is ideal to study the short and long-term responses of TBI in a more human-like model and to study the potential of novel diagnostics and therapeutics to translate successfully to human patients.

Acknowledgments

We would like to thank Richard Utley and Kelly Parham for their animal assistance; Vivian Lau and Lisa Reno for their surgical expertise and support; Mary Kate Mehegan for her assistance with animal work and tissue analysis; and Daniela Lorenco for her statistical analysis assistance. Financial support was provided by the University of Georgia Office of the Vice President for Research.

Author Disclosure Statement

No competing financial interests exist.

References

1. Langlois, J.A., Rutland-Brown, W., Tand homas, K.E. (2006). Traumatic brain injury in the United States: Emergency deparment visits, hospitalizations, and deaths. Centers for Disease Control and Prevention, National Center for Injury Prevention and Control: Atlanta, GA.
2. Schneier, A.J., Shields, B.J., Hostetler, S.G., Xiang, H., and Smith, G.A. (2006). Incidence of pediatric traumatic brain injury and associated hospital resource utilization in the United States. Pediatrics 118, 483–492.
3. Stiles, J. (2000). Neural plasticity and cognitive development. Dev. Neuropsychol. 18, 237–272.
4. Anderson, V., Catroppa, C., Morse, S., Haritou, F., and Rosenfeld, J. (2005). Functional plasticity or vulnerability after early brain injury? Pediatrics 116, 1374–1382.
5. Anderson, V., Godfrey, C., Rosenfeld, J.V., and Catroppa, C. (2012). Predictors of cognitive function and recovery 10 years after traumatic brain injury in young children. Pediatrics 129, e254–e261.
6. Li, L. and Liu, J. (2013). The effect of pediatric traumatic brain injury on behavioral outcomes: a systematic review. Dev. Med. Child Neurol. 55, 37–45.
7. Beretta, E., Cimolin, V., Piccinini, L., Carla Turconi, A., Galbiati, S., Crivellini, M., Galli, M., and Strazzer, S. (2009). Assessment of gait recovery in children after Traumatic Brain Injury. Brain Inj. 23, 751–759.
8. Fakhry, S.M., Trask, A.L., Waller, M.A., Watts, D.D., and IRTC Neurotrauma Task Force (2004). Management of brain-injured patients by an evidence-based medicine protocol improves outcomes and decreases hospital charges. J. Trauma 56, 492–499.
9. Allen, K.A. (2016). Pathophysiology and treatment of severe traumatic brain injuries in children. J. Neurosci. Nurs. 48, 15–27.
10. Maas, A.I., Roozenbeek, B., and Manley, G.T. (2010). Clinical trials in traumatic brain injury: past experience and current developments. Neurotherapeutics 7, 115–126.
11. Xiong, Y., Mahmood, A., and Chopp, M. (2009). Emerging treatments for traumatic brain injury. Expert Opin. Emerg. Drugs 14, 67–84.
12. Stein, D.G., Geddes, R.I., and Sribnick, E.A. (2015). Recent developments in clinical trials for the treatment of traumatic brain injury. Handb. Clin. Neurol. 127, 433–451.
13. Xiong, Y., Mahmood, A., and Chopp, M. (2013). Animal models of traumatic brain injury. Nat. Rev. Neurosci. 14, 128–142.
14. Kobeissy, F.H. (2015). Brain *Neurotrauma: Molecular, Neuropsychological, and Rehabilitation Aspects*. CRC Press, Taylor & Francis Group: Boca Raton.
15. Romine, J., Gao, X.,and Chen, J. (2014). Controlled cortical impact model for traumatic brain injury. J. Vis. Exp. e51781.
16. Bigler, E.D., Abildskov, T.J., Petrie, J., Farrer, T.J., Dennis, M., Simic, N., Taylor, H.G., Rubin, K.H., Vannatta, K., Gerhardt, C.A., Stancin, T., and Owen Yeates, K. (2013). Heterogeneity of brain lesions in pediatric traumatic brain injury. Neuropsychology 27, 438–451.
17. Anderson, V.A., Catroppa, C., Rosenfeld, J., Haritou, F., and Morse, S.A. (2000). Recovery of memory function following traumatic brain injury in pre-school children. Brain Inj. 14, 679–692.
18. Kuhtz-Buschbeck, J.P., Stolze, H., Golge, M., and Ritz, A. (2003). Analyses of gait, reaching, and grasping in children after traumatic brain injury. Arch. Phys. Med. Rehabil. 84, 424–430.
19. Fox, G.B., Fan, L., Levasseur, R.A., and Faden, A.I. (1998). Sustained sensory/motor and cognitive deficits with neuronal apoptosis following controlled cortical impact brain injury in the mouse. J. Neurotrauma 15, 599–614.
20. Saatman, K.E., Feeko, K.J., Pape, R.L. and Raghupathi, R. (2006). Differential behavioral and histopathological responses to graded cortical impact injury in mice. J. Neurotrauma 23, 1241–1253.
21. Yu, S., Kaneko, Y., Bae, E., Stahl, C.E., Wang, Y., van Loveren, H., Sanberg, P.R., and Borlongan, C.V. (2009). Severity of controlled cortical impact traumatic brain injury in rats and mice dictates degree of behavioral deficits. Brain Res. 1287, 157–163.
22. Washington, P.M., Forcelli, P.A., Wilkins, T., Zapple, D.N., Parsadanian, M., and Burns, M.P. (2012). The effect of injury severity on behavior: a phenotypic study of cognitive and emotional deficits after mild, moderate, and severe controlled cortical impact injury in mice. J. Neurotrauma 29, 2283–2296.
23. Zhao, Z., Loane, D.J., Murray, M.G., 2nd, Stoica, B.A., and Faden, A.I. (2012). Comparing the predictive value of multiple cognitive, affective, and motor tasks after rodent traumatic brain injury. J. Neurotrauma 29, 2475–2489.
24. Xiong, Y., Mahmood, A., and Chopp, M. (2010). Neurorestorative treatments for traumatic brain injury. Discov. Med. 10, 434–442.
25. Buki, A., Okonkwo, D.O., and Povlishock, J.T. (1999). Postinjury cyclosporin A administration limits axonal damage and disconnection in traumatic brain injury. J. Neurotrauma 16, 511–521.
26. Riess, P., Zhang, C., Saatman, K.E., Laurer, H.L., Longhi, L.G., Raghupathi, R., Lenzlinger, P.M., Lifshitz, J., Boockvar, J., Neugebauer, E., Snyder, E.Y., and McIntosh, T.K. (2002). Transplanted neural stem cells survive, differentiate, and improve neurological motor function after experimental traumatic brain injury. Neurosurgery 51, 1043–1052.
27. Kolb, B., Gibb, R., and Gorny, G. (2000). Cortical plasticity and the development of behavior after early frontal cortical injury. Dev. Neuropsychol. 18, 423–444.
28. Johnson, V.E., Meaney, D.F., Cullen, D.K., and Smith, D.H. (2015). Animal models of traumatic brain injury. Handb. Clin. Neurol. 127, 115–128.
29. Kandel, E.R. (2013). *Principles of Neural Science,* 5th ed. McGraw-Hill: New York.
30. Ahmad, A.S., Satriotomo, I., Fazal, J., Nadeau, S.E., and Dore, S. (2015). Considerations for the optimization of induced white matter injury preclinical models. Front. Neurol. 6, 172.
31. Thomas, J.M. and Beamer, J.L. (1971). Age-weight relationships of selected organs and body weight for miniature swine. Growth 35, 259–272.
32. Coppoletta, J.M. and Wolbach, S.B. (1933). Body length and organ weights of infants and children: a study of the body length and normal weights of the more important vital organs of the body between birth and twelve years of age. Am. J. Pathol. 9, 55–70.

33. Pond, W.G., Boleman, S.L., Fiorotto, M.L., Ho, H., Knabe, D.A., Mersmann, H.J., Savell, J.W., and Su, D.R. (2000). Perinatal ontogeny of brain growth in the domestic pig. Proc. Soc. Exp. Biol. Med. 223, 102–108.
34. Flynn, T.J. (1984). Developmental changes of myelin-related lipids in brain of miniature swine. Neurochem. Res. 9, 935–945.
35. Lind, N.M., Moustgaard, A., Jelsing, J., Vajta, G., Cumming, P., and Hansen, A.K. (2007). The use of pigs in neuroscience: modeling brain disorders. Neurosci. Biobehav. Rev. 31, 728–751.
36. Zhang, K. and Sejnowski, T.J. (2000). A universal scaling law between gray matter and white matter of cerebral cortex. Proc. Natl. Acad. Sci. U. S. A. 97, 5621–5626.
37. Fairbairn, L., Kapetanovic, R., Sester, D.P., and Hume, D.A. (2011). The mononuclear phagocyte system of the pig as a model for understanding human innate immunity and disease. J. Leukoc. Biol. 89, 855–871.
38. Gale, S.D., Johnson, S.C., Bigler, E.D., and Blatter, D.D. (1995). Nonspecific white matter degeneration following traumatic brain injury. J. Int. Neuropsychol. Soc. 1, 17–28.
39. Lighthall, J.W. (1988). Controlled cortical impact: a new experimental brain injury model. J. Neurotrauma 5, 1–15.
40. Hutchinson, E.B., Schwerin, S.C., Radomski, K.L., Irfanoglu, M.O., Juliano, S.L., and Pierpaoli, C.M. (2016). Quantitative MRI and DTI abnormalities during the acute period following CCI in the ferret. Shock 46, Suppl 1, 167–176.
41. Schwerin, S.C., Hutchinson, E.B., Radomski, K.L., Ngalula, K.P., Pierpaoli, C.M., and Juliano, S.L. (2017). Establishing the ferret as a gyrencephalic animal model of traumatic brain injury: optimization of controlled cortical impact procedures. J. Neuroscience Methods 285, 82–96.
42. King, C., Robinson, T., Dixon, C.E., Rao, G.R., Larnard, D., and Nemoto, C.E. (2010). Brain temperature profiles during epidural cooling with the ChillerPad in a monkey model of traumatic brain injury. J. Neurotrauma 27, 1895–1903.
43. Duhaime, A.C., Margulies, S.S., Durham, S.R., O'Rourke, M.M., Golden, J.A., Marwaha, S., and Raghupathi, R. (2000). Maturation-dependent response of the piglet brain to scaled cortical impact. J. Neurosurg. 93, 455–462.
44. Alessandri, B., Heimann, A., Filippi, R., Kopacz, L.. and Kempski, O. (2003). Moderate controlled cortical contusion in pigs: effects on multi-parametric neuromonitoring and clinical relevance. J. Neurotrauma 20, 1293–1305.
45. Manley, G.T., Rosenthal, G., Lam, M., Morabito, D., Yan, D., Derugin, N., Bollen, A., Knudson, M.M., and Panter, S.S. (2006). Controlled cortical impact in swine: pathophysiology and biomechanics. J. Neurotrauma 23, 128–139.
46. Mytar, J., Kibler, K.K., Easley, R.B., Smielewski, P., Czosnyka, M., Andropoulos, D.B., and Brady, K.M. (2012). Static autoregulation is intact early after severe unilateral brain injury in a neonatal Swine model. Neurosurgery 71, 138–145.
47. Duberstein, K.J., Platt, S.R., Holmes, S.P., Dove, C.R., Howerth, E.W., Kent, M., Stice, S.L., Hill, W.D., Hess, D.C., and West, F.D. (2014). Gait analysis in a pre- and post-ischemic stroke biomedical pig model. Physiol. Behav. 125, 8–16.
48. Schneider, C.A., Rasband, W.S., and Eliceiri, K.W. (2012). NIH Image to ImageJ: 25 years of image analysis. Nat. Methods 9, 671–675.
49. Platt, S.R., Holmes, S.P., Howerth, E.W., Duberstein, K.J., Dove, C.R., Kinder, H.A., Wyatt, E.L., Linville, A.V., Lau, V.W., Stice, S.L., Hill, W.D., Hess, D.C., and West, F.D. (2014). Development and characterization of a Yucatan miniature biomedical pig permanent middle cerebral artery occlusion stroke model. Exp. Transl. Stroke Med. 6, 5.
50. Osier, N. and Dixon, C.E. (2016). The controlled cortical impact model of experimental brain trauma: overview, research applications, and protocol. Methods Mol. Biol. 1462, 177–192.
51. Sindelar, B., Bailes, J.E., Sherman, S.A., Finan, J.D., Stone, J., Lee, J.M., Ahmadian, S., Zhou, Y., Patel, V., and Smith, D. (2016). Effect of Internal jugular vein compression on intracranial hemorrhage in a porcine controlled cortical impact model. J. Neurotrauma 34, 1703–1709.
52. Jin, G., DeMoya, M.A., Duggan, M., Knightly, T., Mejaddam, A.Y., Hwabejire, J., Lu, J., Smith, W.M., Kasotakis, G., Velmahos, G.C., Socrate, S., and Alam, H.B. (2012). Traumatic brain injury and hemorrhagic shock: evaluation of different resuscitation strategies in a large animal model of combined insults. Shock 38, 49–56.
53. Meissner, A., Timaru-Kast, R., Heimann, A., Hoelper, B., Kempski, O., and Alessandri, B. (2011). Effects of a small acute subdural hematoma following traumatic brain injury on neuromonitoring, brain swelling and histology in pigs. Eur. Surg. Res. 47, 141–153.
54. Chastain, C.A., Oyoyo, U.E., Zipperman, M., Joo, E., Ashwal, S., Shutter, L.A., and Tong, K.A. (2009). Predicting outcomes of traumatic brain injury by imaging modality and injury distribution. J. Neurotrauma 26, 1183–1196.
55. Pierallini, A., Pantano, P., Fantozzi, L.M., Bonamini, M., Vichi, R., Zylberman, R., Pisarri, F., Colonnese, C., and Bozzao, L. (2000). Correlation between MRI findings and long-term outcome in patients with severe brain trauma. Neuroradiology 42, 860–867.
56. McGinn, M.J. and Povlishock, J.T. (2015). Cellular and molecular mechanisms of injury and spontaneous recovery. Handb. Clin. Neurol. 127, 67–87.
57. Duhaime, A.C., Hunter, J.V., Grate, L.L., Kim, A., Golden, J., Demidenko, E., and Harris, C. (2003). Magnetic resonance imaging studies of age-dependent responses to scaled focal brain injury in the piglet. J. Neurosurg. 99, 542–548.
58. Missios, S., Harris, B.T., Dodge, C.P., Simoni, M.K., Costine, B.A., Lee, Y.L., Quebada, P.B., Hillier, S.C., Adams, L.B., and Duhaime, A.C. (2009). Scaled cortical impact in immature swine: effect of age and gender on lesion volume. J. Neurotrauma 26, 1943–1951.
59. Wolf, H.K., Buslei, R., Schmidt-Kastner, R., Schmidt-Kastner, P.K., Pietsch, T., Wiestler, O.D., and Blumcke, I. (1996). NeuN: a useful neuronal marker for diagnostic histopathology. J. Histochem. Cytochem. 44, 1167–1171.
60. Buritica, E., Villamil, L., Guzman, F., Escobar, M.I., Garcia-Cairasco, N., and Pimienta, H.J. (2009). Changes in calcium-binding protein expression in human cortical contusion tissue. J, Neurotrauma 26, 2145–2155.
61. Gobbel, G.T., Bonfield, C., Carson-Walter, E.B., and Adelson, P.D. (2007). Diffuse alterations in synaptic protein expression following focal traumatic brain injury in the immature rat. Childs Nerv. Syst. 23, 1171–1179.
62. Ajao, D.O., Pop, V., Kamper, J.E., Adami, A., Rudobeck, E., Huang, L., Vlkolinsky, R., Hartman, R.E., Ashwal, S., Obenaus, A., and Badaut, J. (2012). Traumatic brain injury in young rats leads to progressive behavioral deficits coincident with altered tissue properties in adulthood. J. Neurotrauma 29, 2060–2074.
63. Middeldorp, J. and Hol, E.M. (2011). GFAP in health and disease. Prog, Neurobiol, 93, 421–443.
64. Burda, J.E., Bernstein, A.M., and Sofroniew, M.V. (2016). Astrocyte roles in traumatic brain injury. Exp. Neurol. 275 Pt 3, 305–315.
65. Ziebell, J.M. and Morganti-Kossmann, M.C. (2010). Involvement of pro- and anti-inflammatory cytokines and chemokines in the pathophysiology of traumatic brain injury. Neurotherapeutics 7, 22–30.
66. Sajja, V.S., Hlavac, N., and VandeVord, P.J. (2016). Role of glia in memory deficits following traumatic brain injury: biomarkers of glia dysfunction. Front. Integr. Neurosci. 10, 7.
67. Harish, G., Mahadevan, A., Pruthi, N., Sreenivasamurthy, S.K., Puttamallesh, V.N., Keshava Prasad, T.S., Shankar, S.K., and Srinivas Bharath, M.M. (2015). Characterization of traumatic brain injury in human brains reveals distinct cellular and molecular changes in contusion and pericontusion. J. Neurochem. 134, 156–172.
68. Gaber, Z.B. and Novitch, B.G. (2011). All the embryo's a stage, and Olig2 in its time plays many parts. Neuron 69, 833–835.
69. Flygt, J., Gumucio, A., Ingelsson, M., Skoglund, K., Holm, J., Alafuzoff, I., and Marklund, N. (2016). Human traumatic brain injury results in oligodendrocyte death and increases the number of oligodendrocyte progenitor cells. J. Neuropathol. Exp. Neurol. 75, 503–515.
70. Dent, K.A., Christie, K.J., Bye, N., Basrai, H.S., Turbic, A., Habgood, M., Cate, H.S., and Turnley, A.M. (2015). Oligodendrocyte birth and death following traumatic brain injury in adult mice. PloS One 10, e0121541.
71. Lotocki, G., de Rivero Vaccari, J.P., Alonso, O., Molano, J.S., Nixon, R., Safavi, P., Dietrich, W.D., and Bramlett, H.M. (2011). Oligodendrocyte vulnerability following traumatic brain injury in rats. Neurosci. Lett. 499, 143–148.
72. Kuhtz-Buschbeck, J.P., Hoppe, B., Golge, M., Dreesmann, M., Damm-Stunitz, U., and Ritz, A. (2003). Sensorimotor recovery in children after traumatic brain injury: analyses of gait, gross motor, and fine motor skills. Dev. Med. Child Neurol. 45, 821–828.

73. Duberstein, K.J., Platt, S.R., Holmes, S.P., Dove, C.R., Howerth, E.W., Kent, M., Stice, S.L., Hill, W.D., Hess, D.C., and West, F.D. (2014). Gait analysis in a pre- and post-ischemic stroke biomedical pig model. Physiol. Behav. 125, 8–16.
74. Ochi, F., Esquenazi, A., Hirai, B., and Talaty, M. (1999). Temporal-spatial feature of gait after traumatic brain injury. J. Head Trauma Rehabil. 14, 105–115.
75. Katz-Leurer, M., Rotem, H., Keren, O., and Meyer, S. (2011). The effect of variable gait modes on walking parameters among children post severe traumatic brain injury and typically developed controls. NeuroRehabilitation 29, 45–51.
76. Katz-Leurer, M., Rotem, H., Lewitus, H., Keren, O., and Meyer, S. (2008). Relationship between balance abilities and gait characteristics in children with post-traumatic brain injury. Brain Inj. 22, 153–159.
77. Katz-Leurer, M., Rotem, H., Keren, O., and Meyer, S. (2009). Balance abilities and gait characteristics in post-traumatic brain injury, cerebral palsy and typically developed children. Dev. Neurorehabil. 12, 100–105.
78. Inness, E.L., Howe, J.A., Niechwiej-Szwedo, E., Jaglal, S.B., McIlroy, W.E., and Verrier, M.C. (2011). Measuring balance and mobility after traumatic brain injury: validation of the community balance and mobility scale (CB&M). Physiother. Can. 63, 199–208.
79. Sambasivan, K., Grilli, L., and Gagnon, I. (2015). Balance and mobility in clinically recovered children and adolescents after a mild traumatic brain injury. J. Pediatr. Rehabil. Med. 8, 335–344.
80. Williams, G., Morris, M.E., Schache, A., and McCrory, P.R. (2009). Incidence of gait abnormalities after traumatic brain injury. Arch. Phys. Med. Rehabil. 90, 587–593.
81. Sashindranath, M., Daglas, M., and Medcalf, R.L. (2015). Evaluation of gait impairment in mice subjected to craniotomy and traumatic brain injury. Behav. Brain Res. 286, 33–38.
82. Neumann, M., Wang, Y., Kim, S., Hong, S.M., Jeng, L., Bilgen, M., and Liu, J. (2009). Assessing gait impairment following experimental traumatic brain injury in mice. J. Neurosci. Methods 176, 34–44.
83. Gagnon, I., Swaine, B., Friedman, D., and Forget, R. (2004). Children show decreased dynamic balance after mild traumatic brain injury. Arch. Phys. Med. Rehabil. 85, 444–452.

Address correspondence to:
Franklin D. West, PhD
Regenerative Bioscience Center
Department of Animal and Dairy Science
University of Georgia
Rhodes Center for Animal and Dairy Science
425 River Road
Athens, GA 30602-2771

E-mail: westf@uga.edu